

Parallel resonant inverter with non dissipative snubber used for induction heating

Abstract. This article describes the parallel resonant inverter with the non dissipative snubber that limits commutation overvoltage and enables the energy of parasitic inductances to be returned to the feeding circuit. The use of the non dissipative snubber (auxiliary AC/DC converter) enables the connection of the HF transformer between the inverter output and a parallel resonant circuit as well as the operation of the inverter in the frequency range, ensuring ZVS type switching. The efficiency of the system was also improved.

Streszczenie. W artykule przedstawiono równoległy falownik rezonansowy z pomocniczym przekształtnikiem AC/DC, który ogranicza przepięcia komutacyjne i umożliwia zwrot energii z indukcyjności pasożytniczych do obwodu zasilania. Zastosowanie pomocniczego przekształtnika AC/DC umożliwiłołączenie transformatora HF między wyjście falownika a równoległy obwód rezonansowy oraz pracę falownika w zakresie częstotliwości zapewniających przełączanie typu ZVS. Zwiększonazostała także sprawność układu. (Równoległy falownik rezonansowy do grzania indukcyjnego z niedysympatywnym tłumikiem przepięć).

Keywords: current source inverter, parallel resonant inverter, induction heating, ZVS, lossless snubber.

Słowa kluczowe: falownik prądu, równoległy falownik rezonansowy, grzanie indukcyjne, tłumik przepięć ze zwrotem energii.

Introduction

The operational principles of the parallel resonant inverter with voltage bi-directional (VB) switches (with diodes connected in series with transistors), at negligible parasitic inductances between the inverter and the resonant circuit (Fig. 1a), are generally well-known [1, 2]. For systems of this type, it is possible to use soft commutated switches that turn on at zero voltage (ZVS) or turn off at zero current (ZCS). The type of switches that may be used is determined by their switching frequency f_s (Fig. 1b, 1c). If the switching frequency is greater than the damped resonant frequency f_{dr} of the resonant circuit, ZCS switches may be used. If, on the other hand, $f_s < f_{dr}$, ZVS switches may be used. The damped resonant frequency (if the resonant tank quality factor is sufficiently large) is approximately equal to $f_0 = 1/2\pi\sqrt{L_r C_r}$. The role of VB-ZCS switches may be served by SCR thyristors, which have been used for parallel resonant inverters for a long time now. On the other hand, the use of VB-ZVS switches, intended for frequencies higher than by ZCS switches, has posed some considerable difficulties. These difficulties were related to overvoltage created by parasitic inductances between the inverter and the resonant circuit during commutation processes.

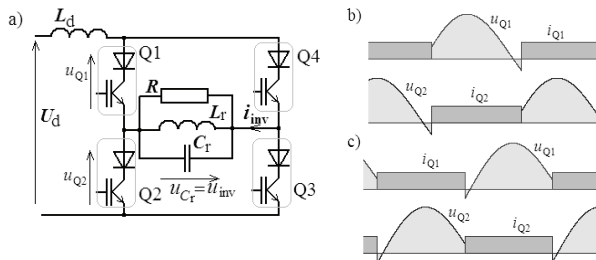


Fig. 1. The schematic diagram of a parallel resonant inverter by neglecting of parasitic inductance between the inverter and the resonant circuit (a) and waveforms of current and voltage of Q1 and Q2 switches for: b) $f_s < f_{dr}$, ZVS switching possible, c) $f_s > f_{dr}$, ZCS switching possible

In many applications, for electrical safety reasons, the inductor has to be separated from the mains. Transformers are used for that purpose. Places where a transformer may be connected to the circuit of this power converter are shown in Fig. 2a. Most commonly, reference sources [1, 3] describe the arrangements with the transformers connected

at places A or B. If the transformer is connected on the mains side (point A) the overall dimensions are large due to low mains frequency (50 Hz).

With the transformer connected at B, the inverter voltage matches the inductor voltage and the transformer is supplied with the voltage of an increased frequency (tens – hundreds kHz). Consequently, the mass of both the winding and the transformer core may be reduced. Since the winding of the transformer constitutes an element of the resonant circuit, the circulation of current of high values in this circuit significantly heats up the winding. Water cooling of the transformer is necessary. This requires a more complex design and increased overall dimensions of the transformer. For water cooling of the primary winding, the separation should be provided by means of an additional transformer at place A.

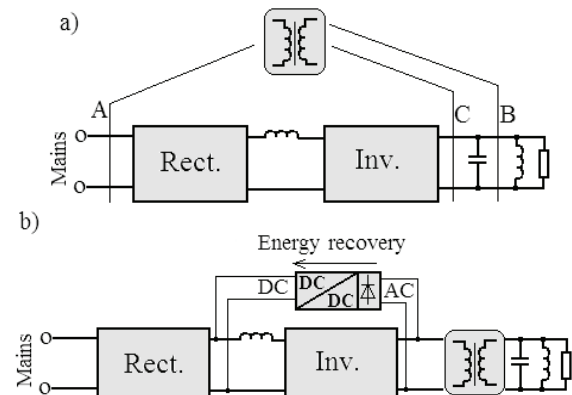


Fig. 2. Schematic diagram of the induction heating system with the current source inverter and the parallel resonant circuit: a) points where the transformer may be connected; b) arrangement with the auxiliary AC/DC converter and the transformer connected between the inverter and the resonant circuit

With the transformer connected at C, the inverter voltage matches the inductor voltage and the transformer is supplied with the voltage of an increased frequency. The mass of both the winding and the transformer core is reduced. The transformer winding is not an element of the resonant circuit and the values of current passing through it are considerably lower than with the transformer connected at B. In this case, the transformer operation should be considered even without water cooling. Therefore, connection of the transformer at C offers certain advantages in terms of its overall dimensions, the mass and

the simplicity of the whole system. However, parasitic leakage inductances of the transformer result in overvoltages, and consequently to losses of energy in semiconductor elements and overvoltage suppressors. The losses become greater with an increase of parasitic inductances and commutated current. In order to limit overvoltages and decrease the consequential losses, an auxiliary AC/DC converter was used. In such an arrangement, unlike in the case of standard overvoltage suppressors, energy is not lost but returned into the feeding circuit of the inverter. The auxiliary AC/DC converter consists of two units: a diode rectifier (AC/DC) and a resonant DC/DC converter [4, 5]. The DC/DC converter transmits the energy to the feeding circuit of the inverter only at the specified value of overvoltage equal to U_{lim} .

The schematic diagram of the induction heating system, including a current source inverter (with VB switches), and a transformer connected between the inverter and a parallel resonant circuit is shown in Fig. 3. In this diagram, the transformer is represented only by leakage inductances (L_{tr}). The parameters and values of the secondary side of the transformer are referred to the primary side.

Operation Principle and Analysis

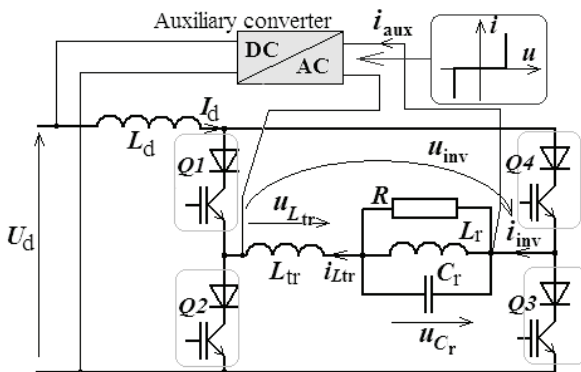


Fig. 3. Schematic diagram of the inverter with the auxiliary AC/DC converter

Figure 4 shows waveforms of current and voltage in the system, including commutation processes, for various switching frequencies of the transistors. Figure 4a illustrates a situation when the commutation occurs before the capacitor C_r voltage wave "goes through zero" ($f_s=1.05f_0>f_{dr}$). Then, conditions exist for the ZCS commutation. Turning off at the ZCS conditions enforces the presence of an inductive snubber at turning on; this role may be served by leakage inductances of the transformer. Figure 4b illustrates a situation when the commutation occurs around the point where the capacitor C_r voltage wave "goes through zero" ($f_s=1.0\cdot f_0 \approx f_{dr}$). Conditions for ZVS and ZCS commutation are not fulfilled. Figure 4c illustrates a situation when the commutation occurs after the capacitor C_r voltage wave "goes through zero" ($f_s=0.97f_0<f_{dr}$). Then, conditions exist for ZVS turning on. The presence of capacitive snubber at turning off is recommended. The role of this type of snubber may be served by self-capacity of switches and input capacity of the auxiliary AC/DC converter.

The use of the auxiliary AC/DC converter is beneficial, regardless of the chosen strategy of the switch control. The converter protects the system against overvoltages when these occur for both ZCS and ZVS switching. If the ZCS control is used, a sudden change of the damped resonant frequency (caused by, for example, introduction of a load or reaching the Curie temperature) may result in a change of the phase shift between the output current and voltage of the inverter and generation of overvoltage.

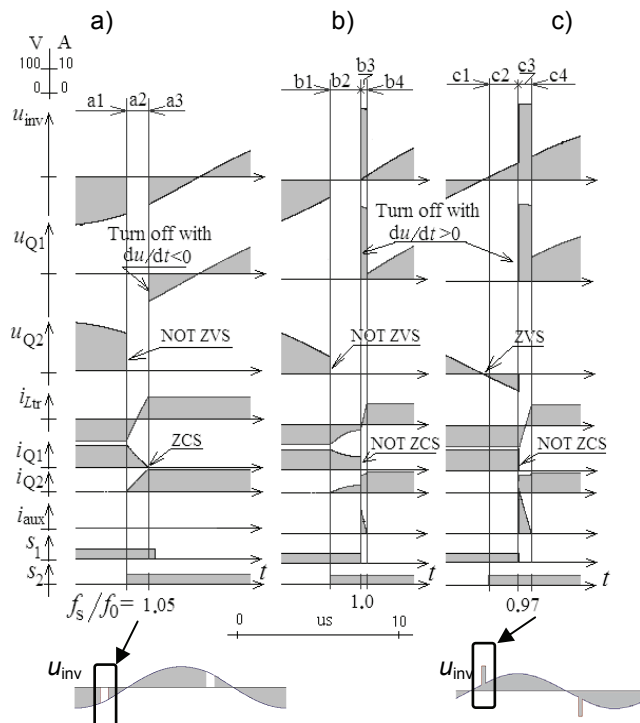


Fig. 4. Waveforms of current and voltage in the inverter for:
a) $f_s = 1.05 \cdot f_0 > f_{dr}$, b) $f_s = 1.0 \cdot f_0 \equiv f_{dr}$, c) $f_s = 0.97 \cdot f_0 < f_{dr}$

Table 1 shows equivalent circuit diagrams of the inverter for time intervals indicated in Figs. 4a - 4c. The conditions fulfilled by current and voltage values of the system in these intervals were also specified. Switching at the frequency $f_s \equiv f_{dr}$ (Fig. 4b) is undesirable since ZVS or ZCS switching is not possible and it may occur only in transient states. What follows, an analysis of operation of the system for conditions illustrated in Figs. 4a and 4c ($f_s > f_{dr}$ and $f_s < f_{dr}$), is presented.

Table 1. Equivalent circuit diagrams of the inverter for various switching frequencies in specific switching operation modes.

a)	$f_s = 1.05 \cdot f_0 > f_{dr}$
Interval a1	$s_1=1, s_2=0, s_3=1, s_4=0,$ $i_{inv}=i_{Ltr}=-I_d < 0, u_{Cr}<0, i_{aux}=0$
Interval a2, begins when: $s_2, s_4 \rightarrow 1$	$s_1=1, s_2=1, s_3=1, s_4=1$ $-I_d \leq i_{inv}=i_{Ltr} \leq I_d, u_{Cr}<0, i_{aux}=0$
Interval a3, begins when: $i_{inv}=i_{Ltr}=I_d$	$s_1=x, s_2=1, s_3=x, s_4=1, (x=0 \text{ or } 1)$ $i_{inv}=i_{Ltr}=I_d, u_{Cr}\leq 0, i_{aux}=0$
b)	$f_s = 1.0 \cdot f_0 \equiv f_{dr}$
Interval b1	$s_1=1, s_2=0, s_3=1, s_4=0,$ $i_{inv}=i_{Ltr}=-I_d, u_{Cr}<0, i_{aux}=0$
Interval b2, begins when: $s_2, s_4 \rightarrow 1$	$s_1=1, s_2=1, s_3=1, s_4=1,$ $-I_d \leq i_{inv}=i_{Ltr} \leq I_d < I_d, u_{Cr}<0 \text{ or } u_{Cr}\geq 0, i_{aux}=0,$
Interval b3 begins when: $s_1, s_3 \rightarrow 0$	$s_1=0, s_2=1, s_3=0, s_4=1$ $I_d < i_{inv}=i_{Ltr} < I_d, i_{inv}=I_d, u_{Cr}<0 \text{ or } u_{Cr}\geq 0, i_{aux}>0$
Interval b4, begins when: $i_{Ltr}=I_d$	$s_1=0, s_2=1, s_3=0, s_4=1$ $i_{inv}=i_{Ltr}=I_d, u_{Cr}>0, i_{aux}=0$

For the adequate high quality factor of the resonant circuit, the shape of voltage u_{Cr} of the capacitor C_r may be regarded as sinusoidal. Further investigation will relate only to such situations when the switching frequency is slightly different from the damped resonant frequency ($f_s \approx f_{dr} \approx f_0$). The input voltage of the inverter, when commutation is not taking place, equals voltage $\pm u_{Cr}$ (Fig. 5). The output voltage during the commutation equals zero at $f_s > f_{dr}$ or voltage U_{lim} (limited by the auxiliary converter) when $f_s < f_{dr}$.

The method for determining the amplitude of the sinusoidal voltage of the resonant capacitor is shown in Fig. 5. The mean input voltage of the inverter equals the feeding voltage:

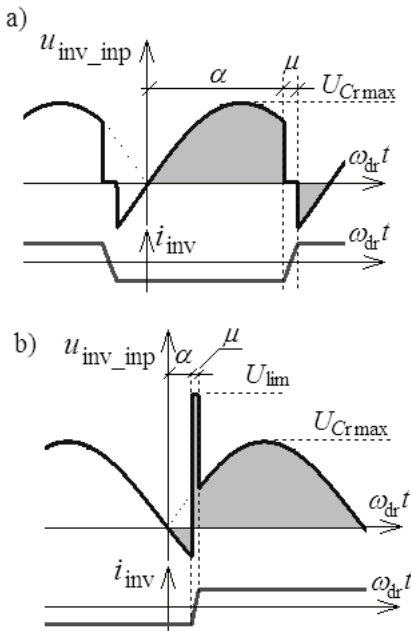


Fig. 5. Waveforms of input voltage and output current of the inverter for various switching frequencies of transistors:
 a) $f_s > f_{dr}$, b) $f_s < f_{dr}$

$$(1) \quad U_d = \frac{1}{\pi} \int_0^{\pi} u_{inv_inp}(\omega_{dr}t) d\omega_{dr} t$$

where $\omega_{dr} = 2\pi f_{dr}$. Therefore, for $f_s > f_{dr}$

$$(2) \quad U_{Crmax} = -\frac{\pi U_d}{[\cos(\alpha + \mu) + \cos \alpha]}$$

and for $f_s < f_{dr}$

$$(3) \quad U_{Crmax} = \frac{\pi U_d}{[\cos(\alpha + \mu) + \cos \alpha + U_{lim} \mu]}$$

The commutation angle μ depends on the value of the commuted current, inductance L_{Tr} and the voltage on this inductance during commutation. It can be determined using the following relation:

$$(4) \quad \Delta i = \frac{1}{L_{Tr}} \int_0^{\mu/\omega_{dr}} u_{L_{Tr}}(t) dt = 2I_d$$

During the commutation, for $f_s > f_{dr}$

$$(5) \quad u_{L_{Tr}} = U_{Crmax} \sin(\omega_{dr}t)$$

On the basis of equation (5):

$$(6) \quad \mu = \arccos(\cos \alpha - \frac{2I_d L_{Tr} \omega_{dr}}{U_{Crmax}}) - \alpha$$

For $\alpha = \pi - \mu$ the commutation ends when $u_{Cr}=0$. With linear approximation of the sine function, the angle is:

$$(7) \quad \mu \approx \sqrt{\frac{4I_d}{\omega_{dr} U_{Crmax}}}$$

For frequency $f_s < f_{dr}$ the voltage on the inductance L_{Tr} is

$$(8) \quad u_{L_{Tr}} = U_{lim} - U_{Crmax} \sin(\omega_{dr}t)$$

Assuming a short duration of commutation in relation to the period of the output voltage of the inverter, the commutation angle may be determined using the approximate relation (9). For $\alpha \approx 0$, the voltage $u_{Cr} \approx 0$ and then the angle is described with the equation (10).

$$(9), (10) \quad \mu \approx \frac{2I_d \omega_{dr} L_{Tr}}{U_{lim} - U_{Crmax} \sin \alpha}, \quad \mu \approx \frac{2I_d \omega_{dr} L_{Tr}}{U_{lim}}$$

The feeding current I_d may be estimated on the basis of equal values of power in the DC circuit and AC circuit:

$$(11) \quad U_d I_d = \frac{1}{\eta} \frac{U_{Crmax}^2}{2R}$$

where: η - estimated efficiency of the system.

Considering the shape of the current i_{aux} (Figs. 3 and 4c), it is possible to determine energy E_{rec} (for each commutation) and power P_{rec} returned to the feeding circuit by the auxiliary AC/DC converter:

$$(12), (13) \quad E_{rec} = U_{lim} I_d \frac{\mu}{\omega_{dr}}, \quad P_{rec} = 4I_d^2 L_{Tr} f_s$$

Formulas (12) and (13) have been devised with an assumption that the commutation begins at the angle $\alpha \approx 0$.

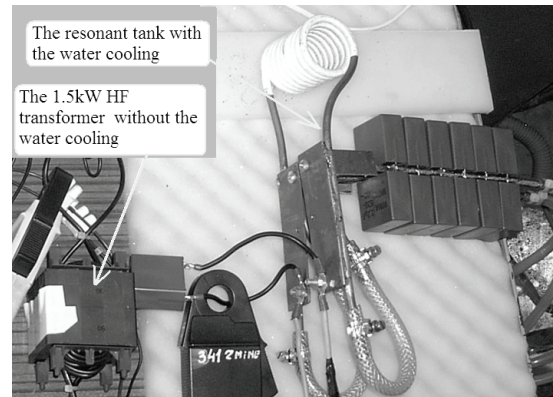


Fig. 6. Elements of the output circuit of the prototype current source inverter used for induction heating

Investigation Results

In order to verify the above assumptions, a laboratory model was built with the transformer placed between the inverter and the parallel resonant circuit (Fig. 6).

For the recovery of energy stored in leakage inductances of the transformer, the AC/DC converter was used. It was constructed as a resonant DC/DC converter [4, 5] (with the constant transformation coefficient) with the rectifier at input.

Figure 7 shows oscilloscope photographs that illustrate waveforms of voltage and current in the system, for: $U_d = 192$ V, $I_d = 7.58$ A, direct current returned by the AC/DC converter $I_{drec} = 0.84$ A, $U_{lim} = 2U_d$, $f_s = 24$ kHz. Power delivered to the primary winding of the transformer reached approx.

1250 W; power returned to the feeding circuit – $P_{\text{rec}} = 160\text{W}$ and power at the inverter input $U_d \cdot I_d = 1455\text{W}$ (Fig. 7 and 8). The efficiency of the inverter with standard overvoltage suppressor, under the very same conditions as shown in the oscillogram in Fig. 7, was approx. 85%. When the standard suppressor was replaced with the energy recovery converter, efficiency improved to approx. 95%.

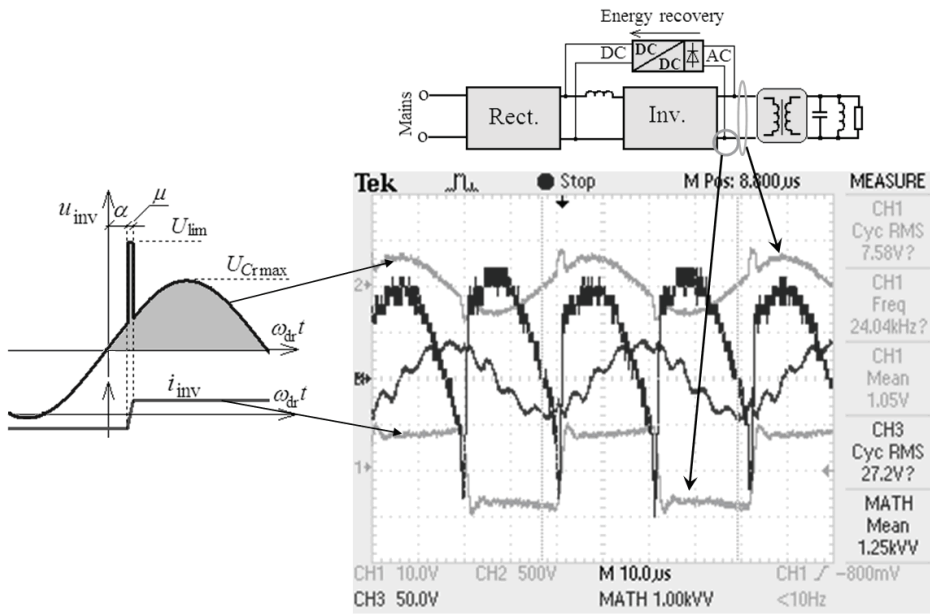


Fig. 7. Waveforms of instantaneous currents, voltage and power in the experimental system:
CH1 = $i_{L\text{Tr}}$ 10 A/div, CH2 = u_{inv} 500 V/div, CH3 = inductor current 650 A/div, MATH = CH1*CH2 = 1 kW/div

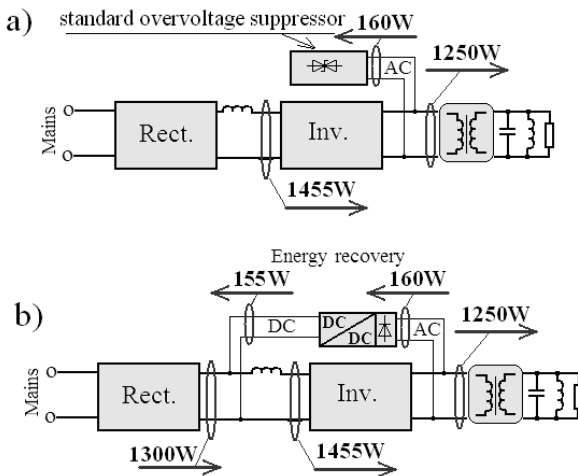


Fig. 8. The values of the power measured in the experimental system

Conclusion

The arrangement of the current source inverter (with auxiliary AC/DC converter) described herein enabled connection of the transformer between the inverter (with transistors operating as ZVS switches) and the parallel

resonant circuit. The enhanced efficiency of the inverter with the auxiliary AC/DC converter was due to the fact that instead of being lost in standard overvoltage suppressors, the energy was returned to the feeding circuit. The transformer (separating the inductor from the feeding circuit) connected between the inverter and the resonant tank, generated less heat than a similar transformer within the resonant circuit. Positive results of the experiments show that the theoretical assumptions were correct. In the future, prototype systems of much greater power will be built and tested. The design of the inverter (with the auxiliary AC/DC converter) described herein may be used as an alternative to systems with parallel resonant circuit supplied by the voltage source inverter through additional inductive elements as described in the reference sources [6, 7].

REFERENCES

- [1] Dede E.J., Jordan J., et al., Conception and Design of a Parallel Resonant Converter for Induction heating, *6th Applied Power Electronics Conference and Exposition*, (1991), 38-44.
- [2] Citko T., Tunia H., Winiarski B., Resonant Circuits in the Power Electronics (Układy rezonansowe w energoelektronice), Wydawnictwa Politechniki Białostockiej, (2001).
- [3] Jordan J., Magraner J.M., et al., Short-Circuit Critical Frequency for Induction Heating Parallel Resonant Inverters, *13th European Conference on Power Electronics and Applications* (2009), 1-9.
- [4] Mućko J., Langer H.G., Bendien J.Ch., A Novel Resonant DC to DC Converter with High Power Density and High Efficiency, *3rd European Conference on Power Electronics and Applications*, (1989), 1467-1471.
- [5] Mućko J., The control methods of series resonant inverters which make possible the simultaneous work of transistors as the ZVS and the "almost ZCS" switches, *Electrical Review*, (Metody sterowania szeregowego falownika rezonansowego zapewniające jednoczesną komutację ZVS i „prawie ZCS”, *Przegląd Elektrotechniczny* No 6, (2010), 137-142.
- [6] Schöönknecht A., De Doncker R., Novel Topology for Parallel Connection of Soft-Switching High-Power High-Frequency Inverters, *IEEE Transactions on Industry Applications*, Vol. 39, (2003), 550 - 555
- [7] Dzieniakowski M. A., Fabianowski J., Ibach R., LCL-Load Modular Converter For Induction Heating, *13th Conference EPE-PEMC*, (2008), 2082 - 2086

Author: Ph.D.Eng. Jan Mućko, University of Technology and Life Sciences, Institute of Electrical Engineering, 7 Prof. S. Kaliskiego, 85-796 Bydgoszcz, Poland,
E-mail: mucko@utp.edu.pl;